

## Supplementary Figures: Automated analysis of single cells in microfluidic traps<sup>†</sup>

Stefan A. Kobel,<sup>a</sup> Olivier Burri,<sup>b</sup> Alexandra Griffa,<sup>b,c</sup> Mukul Girotra,<sup>a</sup> Arne Seitz,<sup>b</sup> and Matthias P. Lutolf<sup>\*a</sup>

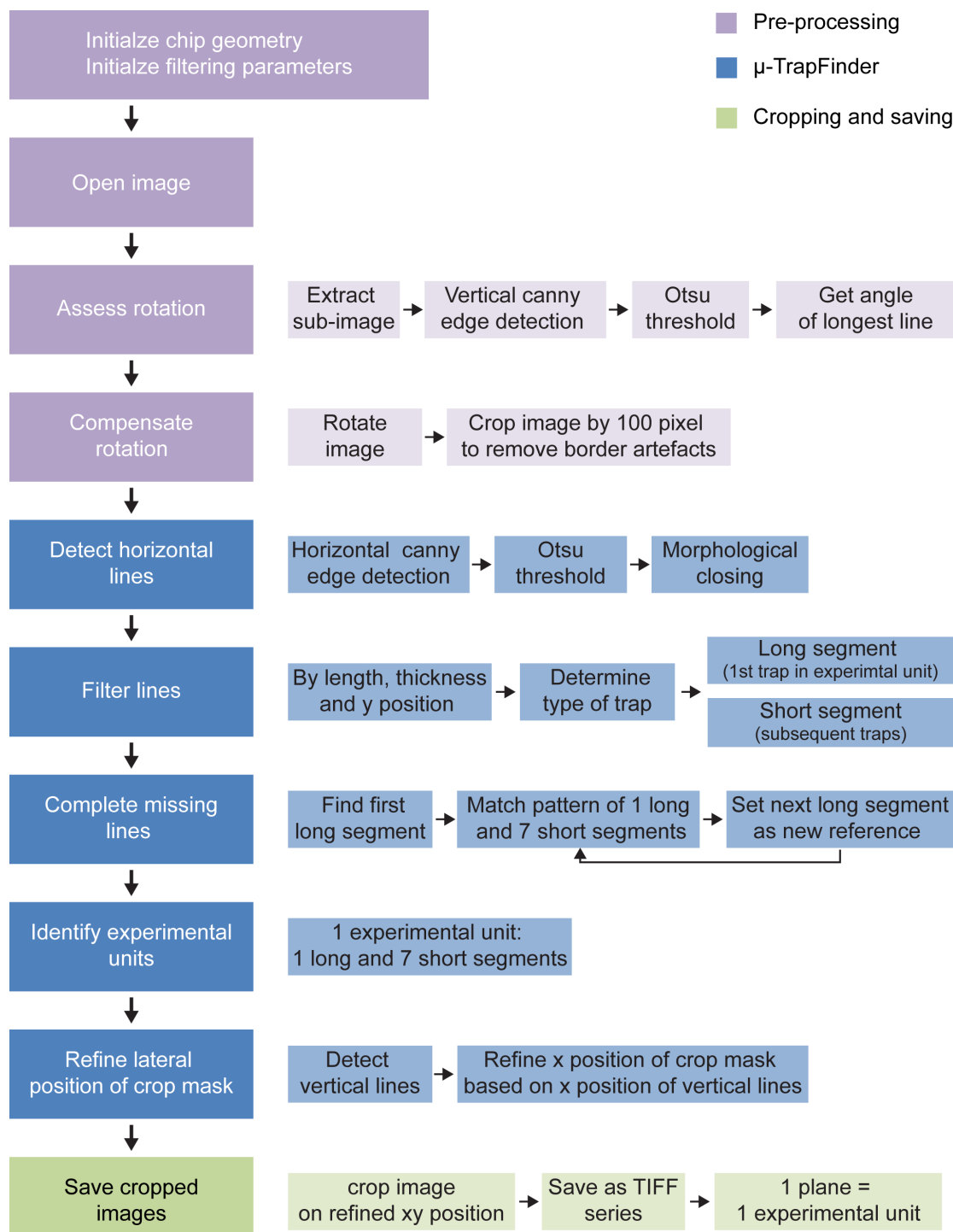
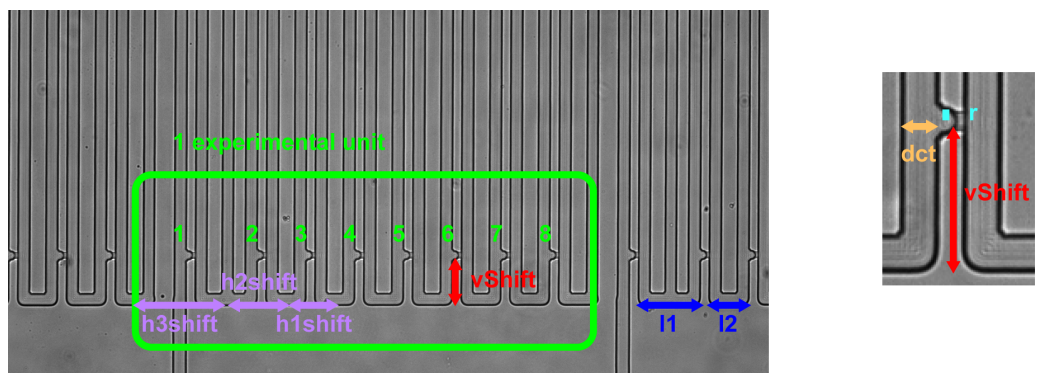


Figure S1: Detailed description of the presented algorithm to detect and mask single cell traps. The algorithm consists of three parts (pre-processing, the μ-TrapFinder and the final cropping and saving). The boxes on the right side provide a more detailed description of the implementation.

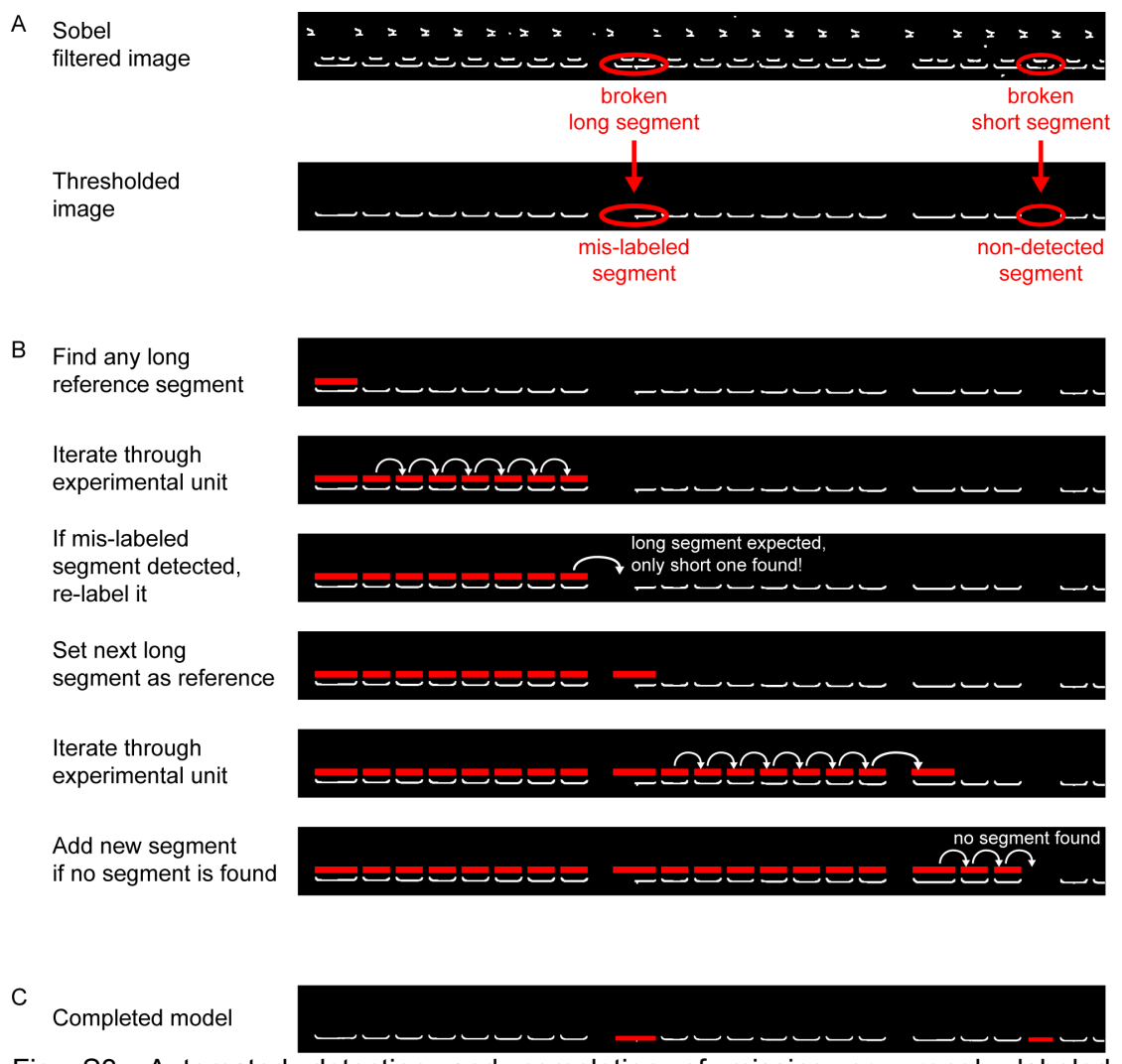


**r** = 5; radius of the trap  
**vShift** = 40; vertical shift between the center of the segment and the center of the trap  
**h1Shift** = 21; horizontal shift between the center of the segment and the center of the trap (for n = 2 to 7)  
**h2Shift** = 30; horizontal shift between the center of the segment and the center of the trap (for n = 1)  
**h3Shift** = 21; horizontal shift between the center of the segment and the center of the trap (for n = 8)

**I1** = 33; length of the short horizontal segment  
**I2** = 53; length of the long horizontal segment  
**dct** = 13; distance between the vertical line of the channel and the center of the trap

All values are in pixels

Fig. S2: Example of the parameters used to detect the single cell traps.



C Completed model



Fig. S3: Automated detection and completion of missing or wrongly labeled segments.

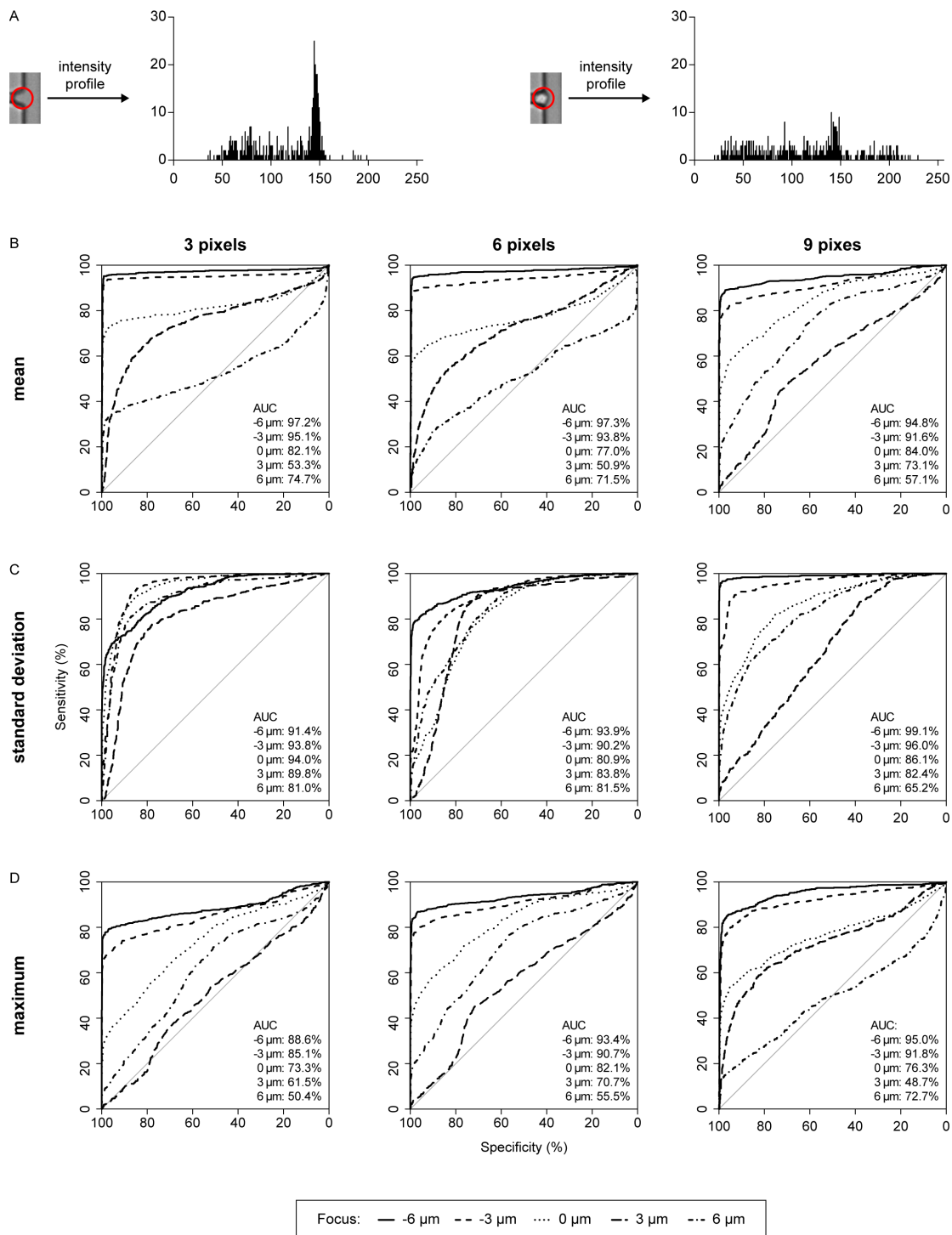


Figure S4: Use of different pixel statistics to detect single cells. (A) We tested the mean, standard deviation and the maximum of the pixel intensities in the single cell traps with differently sized measurement masks and at different focal positions. In order to detect the presence of cell in the trap, thresholds were chosen that were above the mean, standard deviation or maximum intensities, respectively of empty traps. Interestingly, this statistical analysis was for highly predictive for the presence of cells in the traps as evidenced by the receiver-operator-characteristics for the mean intensity (B), standard deviation (C) and maximum of the pixel intensities (D) for different measurement areas. As a consequence, sensitivities of 95% and specificities of even 99% could be achieved (e.g. for 3-pixel mean and 9-pixel standard deviation measurements, data not shown).

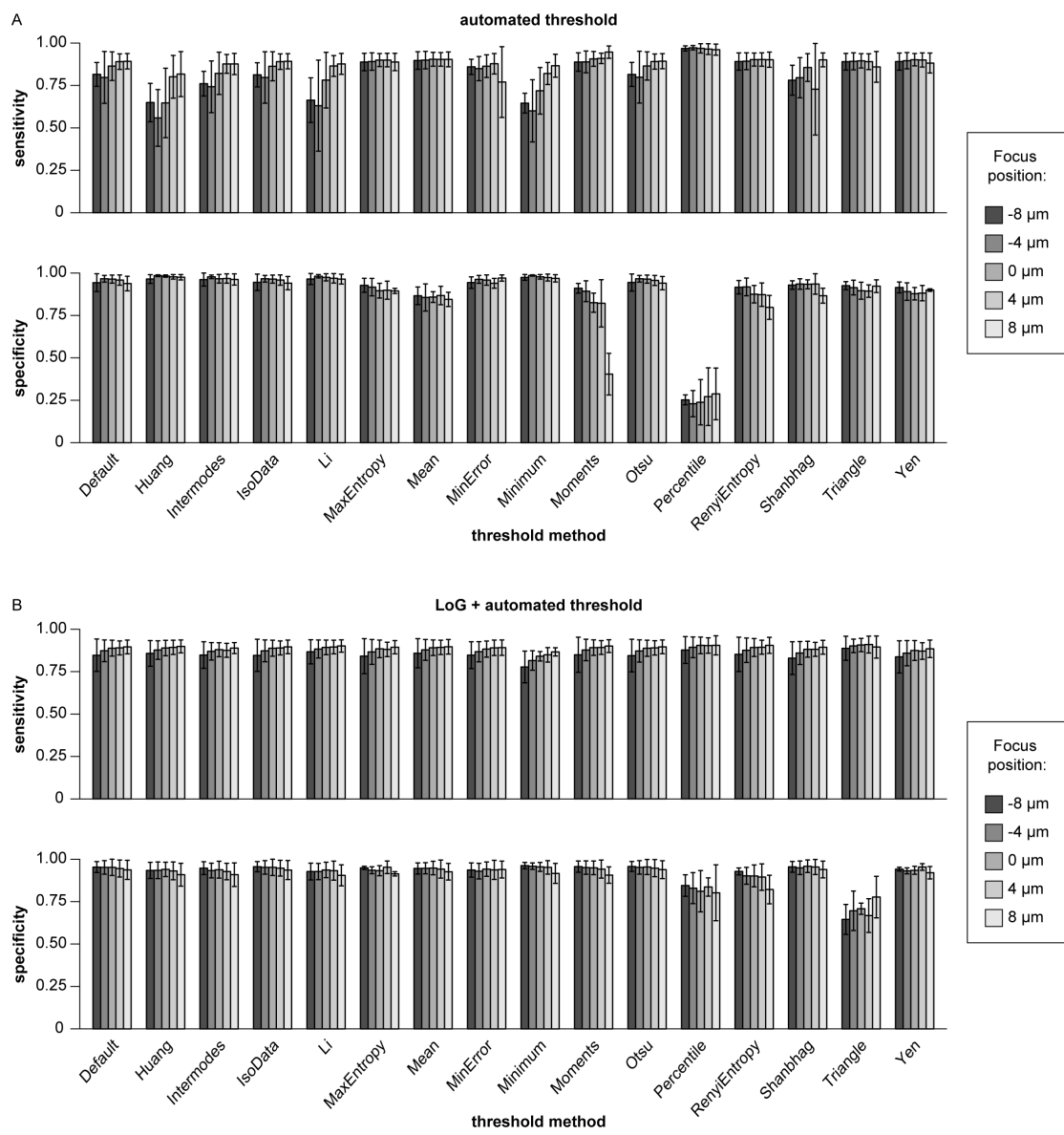


Figure S5: Automated detection of single cells in microfluidic single cell trap. (A) Combinatorial testing of different thresholding algorithms and focus position to segment cells. Many combinations yielded in very high sensitivities and specificities. Interestingly, some of the algorithms are less sensitive at above-focus positions. This difference is mostly lost when the images are treated with a LoG filter before thresholding (B).

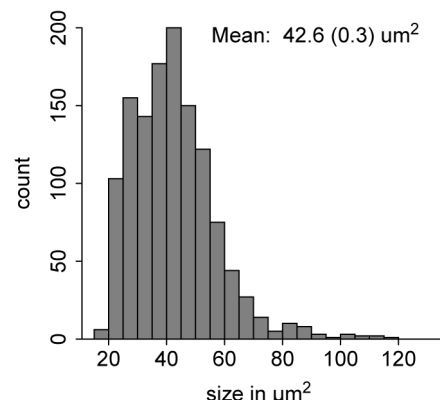


Figure S6: Measurement of single cell size. The average size of the trapped cells (approximately  $42 \mu\text{m}^2$ ) corresponded well to the expected size of HSCs that have a diameter of about  $7 \mu\text{m}$ .